Published in final edited form as:
Arch Neurol. 2011 February ; 68(2): 232–240. doi:10.1001/archneurol.2010.357.

In Vivo Fibrillar β-Amyloid Detected Using [^{11}C]PiB Positron Emission Tomography and Neuropathologic Assessment in Older Adults

Dr. Jitka Sojkova, MD, **Dr. Ira Driscoll, PhD**, **Dr. Diego Iacono, MD, PhD**, **Dr. Yun Zhou, PhD**, **Dr. Kari-Elise Codispoti, MD**, **Dr. Michael A. Kraut, MD, PhD**, **Dr. Luigi Ferrucci, MD, PhD**, **Dr. Olga Pletnikova, MD**, **Dr. Chester A. Mathis, PhD**, **Dr. William E. Klunk, MD, PhD**, **Dr. Richard J. O'Brien, MD, PhD**, **Dr. Dean F. Wong, MD, PhD**, **Dr. Juan C. Troncoso, MD**, and **Dr. Susan M. Resnick, PhD**

National Institute on Aging, National Institutes of Health, Baltimore, Maryland (Drs Sojkova, Driscoll, Ferrucci, and Resnick); Russell H. Morgan Department of Radiology and Radiological Sciences (Drs Sojkova, Zhou, Codispoti, Kraut, and Wong) and Departments of Pathology (Drs Iacono, Codispoti, Pletnikova, and Troncoso), Neurology (Dr Troncoso), and Psychiatry (Dr Wong), The Johns Hopkins University School of Medicine, Baltimore; Departments of Radiology (Dr Mathis) and Psychiatry (Dr Klunk), University of Pittsburgh, Pittsburgh, Pennsylvania; Department of Neurology, The Johns Hopkins Bayview Medical Center, Baltimore (Dr O'Brien); and Department of Environmental Health Sciences, The Johns Hopkins University Bloomberg School of Public Health, Baltimore (Dr Wong)

Abstract

Background—In demented older adults, in vivo amyloid imaging shows agreement with diagnostic neuropathologic assessment of β-amyloid (Aβ). However, the extent of agreement in nondemented older adults remains unclear.

Objective—To compare Aβ quantified using in vivo carbon 11–labeled Pittsburgh Compound B positron emission tomography and postmortem neuropathologic assessment of Aβ in older adults.

Design—Case series.

Setting—Community-dwelling older adults who came to autopsy.

Participants—Five nondemented and 1 demented participant from the Baltimore Longitudinal Study of Aging.

Correspondence: Susan M. Resnick, PhD, Laboratory of Behavioral Neuroscience, Biomedical Research Center, National Institute on Aging, National Institutes of Health, 251 Bayview Blvd, Room 4B317, Baltimore, MD 21224 (resnicks@grc.nia.nih.gov).

Author Contributions: All authors had full access to all the data in the study and take responsibility for the integrity of the data and the accuracy of the data analysis. *Study concept and design:* Sojkova, Kraut, Klunk, and Resnick. *Acquisition of data:* Iacono, Codispoti, Pletnikova, O'Brien, Wong, Troncoso, and Resnick. *Analysis and interpretation of data:* Sojkova, Driscoll, Zhou, Kraut, Ferrucci, Mathis, Klunk, O'Brien, Wong, and Resnick. *Drafting of the manuscript:* Sojkova, Zhou, and Wong. *Critical revision of the manuscript for important intellectual content:* Driscoll, Iacono, Codispoti, Kraut, Ferrucci, Pletnikova, Mathis, Klunk, O'Brien, Troncoso, and Resnick. *Obtained funding:* Kraut, O'Brien, Troncoso, and Resnick. *Administrative, technical, and material support:* Sojkova, Driscoll, Iacono, Pletnikova, Wong, and Resnick. *Study supervision:* Ferrucci, O'Brien, Wong, and Resnick.

Financial Disclosure: GE Healthcare holds a license agreement with the University of Pittsburgh based on the PiB technology described in this article. Drs Klunk and Mathis are coinventors of PiB and, as such, have a financial interest in this license agreement.

Additional Contributions: We thank the BLSA participants and their families for making this study possible; Andrew Crabb, MS, for image data management, Beth Nardi, MA, for study management; and the staff of the PET facility, the Brain Bank, and the Autopsy Study at The Johns Hopkins University and the neuroimaging staff of the National Institute on Aging for their assistance.

Main Outcome Measure—Agreement between the mean cortical distribution volume ratio and the Consortium to Establish a Registry for AD (CERAD) neuritic plaque (NP) score used for pathologic diagnosis of Alzheimer disease.

Results—Of the 6 participants, 4 had moderate NPs, 2 had sparse or no detectable NPs, and 3 had microscopic findings of cerebral amyloid angiopathy at autopsy. On in vivo imaging, the mean cortical distribution volume ratio ranged from 0.96 to 1.59. Although there was agreement between in vivo amyloid imaging and CERAD NP scores in participants with either high or negligible Aβ levels in vivo, only limited agreement was observed among those with intermediate levels of Aβ. The best overall agreement was achieved at a distribution volume ratio of 1.2.

Conclusions—In older adults, variable agreement between in vivo imaging and CERAD NP score was observed. The limited agreement may, in part, reflect differences in typical measurements of Aβ using imaging compared with the CERAD neuropathologic protocol. Direct quantification of regional Aβ in relation to in vivo imaging is necessary to further enhance our understanding of the imaging–pathologic assessment correlation.

Positron emission tomography (PET) amyloid imaging agents, such as carbon 11–labeled Pittsburgh Compound B ([^{11}C]PiB), have facilitated in vivo evaluation of cerebral amyloidosis,[1] including detection of fibrillar β-amyloid (Aβ) in diffuse, cored, and neuritic (NP) plaques[1,2] and in blood vessels in cerebral amyloid angiopathy (CAA).[1–3] Brain biopsies of patients with symptomatic normal-pressure hydrocephalus[4] and postmortem evaluation of 2 demented patients[2,5] demonstrated good overall agreement between [^{11}C]PiB imaging and Aβ load detected by means of immunohistochemical analysis or the age-based, semiquantitative Consortium to Establish a Registry for AD (CERAD) scale.[6] However, recent articles have also described a case of sparse NPs in a demented older adult with negligible [^{11}C]PiB retention[7] and an example of an elevated Aβ level by means of immunohistochemical analysis in an individual with a [^{11}C]PiB distribution volume ratio (DVR) of 1.2.[4] Thus, the extent of agreement between in vivo [^{11}C]PiB imaging and neuropathologic assessment remains unclear, especially in nondemented older adults who have lower Aβ loads and greater variability in Aβ levels.[8]

To investigate the relation between [^{11}C]PiB imaging and CERAD-based neuropathologic diagnosis of Alzheimer disease (AD) lesions, we evaluated 5 nondemented and 1 demented participant from the Neuroimaging Substudy of the Baltimore Longitudinal Study of Aging (NI-BLSA)[9] who underwent in vivo [^{11}C]PiB imaging and postmortem evaluation. We also investigated the [^{11}C]PiB-positive threshold that maximizes agreement between in vivo Aβ imaging and CERAD NP scores and related it to the level at which Aβ is detectable by [^{11}C]PiB imaging. We then examined cases with limited agreement to identify factors that affect interpretation of in vivo Aβ imaging relative to neuropathologic assessment.

METHODS

STUDY PARTICIPANTS

Participants in the NI-BLSA[9] with [^{11}C]PiB imaging and postmortem neuropathologic evaluation were included. Cognitive status was determined by consensus diagnosis according to established procedures[10,11] using the Clinical Dementia Rating (CDR) Scale[12] and a battery of neuropsychological tests administered at each visit. None of the participants had Parkinson disease, brain tumor, epilepsy, or clinical stroke at the time of [^{11}C]PiB PET. Written informed consent was obtained from participants at each visit. Institutional review boards overseeing The Johns Hopkins Medical Institutions and the National Institute on Aging approved the BLSA and the neuroimaging and autopsy evaluations.

NEUROPSYCHOLOGICAL TESTING

Participants were evaluated annually via a battery of 12 neuropsychological tests during a mean (SD) of 11.7 (0.9) years before the first PiB study. Tests included the Mini-Mental State Examination as a measure of mental status; the California Verbal Learning Test and the Benton Visual Retention Test to assess verbal and visual memory; the Trail Making Test Part A to measure attention; and the Trail Making Test Part B, category (animals, fruits, and vegetables) and letter fluency, and the Boston Naming Test to evaluate executive and language functions.

[^{11}C]PiB STUDIES

Dynamic [^{11}C]PiB PET was performed using a GE Advance scanner (GE Healthcare, Waukesha, Wisconsin) in 3-dimensional mode. We started PET immediately after intravenous bolus injection of a mean (SD) of 14.5 (2.1) mCi of [^{11}C]PiB with a mean (SD) specific activity of 4.12 (1.59) Ci/μmol (range, 1.9–6.3 Ci/μmol) in the 5 nondemented participants (participants A–E). The participant who became demented (participant F) had 3 [^{11}C]PiB scans during the regular follow-up intervals with a mean (SD) of 14.5 (2.1) mCi of [^{11}C]PiB with a mean (SD) specific activity of 6.56 (3.2) Ci/μmol (range, 3.8–10.1 Ci/μmol). Transmission scans in 2-dimensional mode using a germanium-68 source were used for attenuation correction. Dynamic images were reconstructed using filtered back projection with a ramp filter (image size=128×128, pixel size=2×2 mm, and section thickness=4.25 mm), yielding a spatial resolution of approximately 4.5-mm full-width at half maximum at the center of the field of view. Custom-fitted thermoplastic masks were used to minimize head motion during scanning. The interval between the last imaging evaluation and the neuropathologic assessment ranged from 0.2 to 2.4 years.

MAGNETIC RESONANCE IMAGING–BASED REGION OF INTEREST DEFINITION

Spoiled gradient recalled magnetic resonance images (MRIs) (124 sections, image matrix=256×256, pixel size=0.94×0.94 mm, and section thickness=1.5 mm) were coregistered to the mean of the first 20-minute dynamic PET images using the mutual information method in the Statistical Parametric Mapping software (SPM2; Wellcome Department of Cognitive Neurology, London, England). Except for 1 claustrophobic participant in whom structural MRI was performed 10 years before baseline [^{11}C]PiB PET, MRIs were obtained in conjunction with PET. In addition to the cerebellum, 15 regions of interest and 3 regions used in CERAD assessment (ie, the middle frontal gyrus, inferior parietal lobule, and superior and middle temporal gyri [SMTG]) were manually drawn on coregistered MRIs.[13]

IN VIVO QUANTIFICATION OF Aβ

The DVRs of regions of interest were estimated by simultaneously fitting a simplified reference tissue model, with the cerebellum as the reference region, to the 18 measured region of interest time activity curves using a linear regression and spatial constraint algorithm[14] applied to data between 0 and 70 minutes. Parametric DVR images for voxelwise analysis calculated using the simplified reference tissue model and linear regression with spatial constraints[14,15] were spatially normalized using an R1 template ($R_1=K_1/K_1$ [reference tissue], the target to reference tissue ratio of tracer transport rate constant from vascular space to tissue).[14]

In addition to the mean and highest regional DVRs of 8 cortical regions (orbitofrontal, prefrontal, superior frontal, parietal, lateral temporal, occipital, and anterior and posterior cingulate), DVRs of 3 regions used in CERAD assessment were also determined. Surface

projections of parametric DVR maps were generated using MRIcro[16] to illustrate sampled regions during CERAD assessment.

NEUROPATHOLOGIC EVALUATION

The brains were examined postmortem in the Division of Neuropathology of The Johns Hopkins University. The left hemi-brain was fixed in 10% buffered formaldehyde for at least 2 weeks and then was sectioned in the coronal plane. Tissue blocks from the middle frontal gyrus, inferior parietal lobule, SMTG, visual cortex, amygdala, and entorhinal cortex were processed, embedded in paraffin, cut at 10 μm, and stained using the Hirano modification of the Bielschowsky silver stain.[6,17] The NP burden was assessed on a semiquantitative age-adjusted scale (CERAD 0, A, B, or C) based on the middle frontal gyrus, inferior parietal lobule, and SMTG.[6] Because all individuals were older than 75 years, the CERAD rating was simplified as follows: 0 indicates no NPs; A, sparse NPs; B, moderate NPs; and C, frequent NPs. In addition, we used unbiased stereologic analysis (fractional area) to estimate the burden of Aβ (6E10; Covance Inc, Princeton, New Jersey) (1:500) immunoreactivity in 5 random, systematically selected paraffin sections from the precuneus. Detailed evaluation of participant E also included evaluation of Aβ plaques on thioflavin S–stained sections. Neurofibrillary tangle stage was assigned a score (0-VI) according to the method of Braak and Braak.[18] The presence of CAA was assessed in regions used for CERAD evaluation on hematoxylin-eosin stains. Evaluation for Lewy body abnormalities was performed.[19]

AMYLOID IMAGING AND DIAGNOSTIC NEUROPATHOLOGIC ASSESSMENT

The primary outcome measure was overall agreement between CERAD NP score and mean cortical DVR (cDVR). We also examined agreement between CERAD NP score and the highest regional DVR and DVRs in the regions used in CERAD assessment. The CERAD ratings were dichotomized into elevated (moderate or frequent) and low (no or sparse) NPs.[11] Cortical DVR thresholds of 1.2, 1.3, and 1.4[8,20] were used as cutoff points to determine agreement with the CERAD plaque rating, CAA, and overall agreement (using the CERAD and CAA), respectively.

RESULTS

STUDY PARTICIPANTS

Demographic and genotype data are given in Table 1. Participants were 78 years and older at the time of [^{11}C]PiB imaging and 80 years and older at death. Two of 6 participants were heterozygous carriers of the apolipoprotein E ε4 allele. Participant D likely experienced a stroke in the interval between in vivo imaging and death because a 4.5×3.0-cm region of encephalomalacia in the left inferior frontal gyrus and because thalamic and basal ganglia lacunar infarcts were found on postmortem evaluation but not on antemortem MRI. All the participants had MRI findings consistent with small-vessel ischemic disease.

COGNITIVE STATUS AND TEST PERFORMANCE

At the time of initial imaging, all the participants were free of dementia, and none had a consensus diagnosis of mild cognitive impairment. Nevertheless, mild memory declines were documented by informant CDR=0.5 in participants D and F (F1 and F2). Participant F, who had 3 serial [^{11}C]PiB evaluations, was normal by consensus diagnosis but had CDR=0.5 at the first PiB scan. His CDR–Sum of Boxes score increased from 0.5 at baseline cognitive assessment a decade before the first PiB scan to 2 at the first PiB scan and 4.5 (CDR=1 and dementia diagnosis) at the last imaging evaluation 55 days before death (Figure 1). Neuropsychological performance was consistent with the CDR in all individuals. The

slope of the California Verbal Learning Test during a mean (SD) of 11.7 (0.9) years before the [^{11}C]PiB study, reflecting longitudinal decline in verbal episodic memory, best differentiated individuals with subtle cognitive decline on the CDR (Table 1). Consistent with a clinical diagnosis of dementia and a neuropathologic diagnosis of probable AD, participant F's initial mild memory deficit progressed during 3-year follow-up to marked deficits in memory, executive function, and language.

IN VIVO Aβ DEPOSITION

Mean cDVRs ranged from 0.96 to 1.59. The highest regional DVR values were observed in the precuneus/posterior cingulate region in 5 of 6 participants and in the superior frontal region in the remaining individual (Table 2 and Figure 2). The DVRs in regions of CERAD assessment are shown in Figure 3.

Participant F, who showed cognitive decline by CDR beginning in 1996, had elevated PiB retention at baseline, with a mean cDVR of 1.54 in 2005 increasing to 1.59 by 2007 and stabilizing at 1.57 in 2008 at the time of dementia diagnosis (Figure 1).

DIAGNOSTIC NEUROPATHOLOGIC ASSESSMENT

Four individuals had moderate NPs (CERAD B), 1 had sparse NPs (CERAD A), and 1 had no NPs (CERAD 0) (Figure 4). Three of the 6 participants had CAA. In 1 participant with CERAD A, Lewy bodies were noted in brainstem and amygdala. Accounting for clinical status (Table 1), the final clinicopathologic CERAD diagnoses were as follows: 1, probable AD; 3, possible AD; and 2, normal.

AGREEMENT BETWEEN IN VIVO Aβ IMAGING AND NEUROPATHOLOGIC ASSESSMENT

Case-Based Evaluation—We found good agreement between imaging and neuropathologic assessment in the individuals with the lowest and highest cDVR values (Figures 2 and 4). The participant with the highest cDVR of 1.59 had a CERAD plaque rating of B and met the criteria for probable AD. All 3 [^{11}C]PiB studies in this participant, including those obtained before the participant developed dementia, showed diffusely elevated cDVRs, in agreement with the CERAD plaque score (Figures 1 and 4).

In contrast, the 3 participants with mean cDVR values less than 1.1 had moderate NPs in at least 1 of the 3 regions routinely sampled for neuropathologic assessment (Figures 2 and 4, participants B-D). Also, CAA was noted in 1 of these individuals (Figure 4, participant D). In addition, detailed evaluation of the participant with an elevated mean cDVR greater than 1.4 but only sparse NPs revealed many diffuse plaques and a high Aβ load on immunostaining not only in the SMTG but also in the precuneus (Figure 5 and Figure 6). The precuneus, which is not routinely included in diagnostic neuropathologic assessment,[6] accounted for the highest [^{11}C]PiB signal in this participant (Figures 2 and 5). Vascular Aβ was also found on neuropathologic evaluation in this participant (Figure 4).

Standard Measures of [^{11}C]PiB Retention in Relation to Diagnostic Neuropathologic Assessment—Using mean cDVR as the measure of in vivo Aβ load, agreement between [^{11}C]PiB at 3 different PiB+ thresholds and CERAD rating was observed in only 2 of 6 participants, A and F (Table 3 and Figures 2 and 4, participants A and F). When CAA was considered with CERAD rating, agreement with mean cDVR remained limited (Table 3). However, when highest regional DVR rather than mean cDVR was used, the best overall agreement was obtained using a PiB+ threshold of a DVR of 1.2, with 5 of the 6 participants showing agreement between [^{11}C]PiB and combined CERAD plaque scores and CAA findings. In addition, good overall agreement between in vivo [^{11}C]PiB imaging and CAA was observed at multiple PiB cutoff levels.

The only case in which agreement between in vivo imaging and pathologic findings was not reached even at a DVR of 1.2 and after accounting for CAA is in participant B. This individual with moderate CERAD and no CAA had a cDVR of 1.01, with the highest DVR of 1.16 in the posterior cingulate gyrus. Participant E, on the other hand, had only sparse NPs on CERAD rating despite a high cDVR. Diffuse plaques were found in the precuneus and the SMTG in this participant, who also had CAA (Figures 2, 4, and 5). Participants C and D had low cDVRs but CERAD B scores, indicating moderate NPs (Figures 2 and 4), but once either the highest DVR or CAA was taken into consideration, agreement was reached at a DVR of 1.2.

[^{11}C]PiB Retention in CERAD Regions in Relation to Diagnostic Neuropathologic Assessment—Associations between regional CERAD and DVR scores show similar patterns as global measures, with overall agreement in 5 of 6 participants at a DVR of 1.2 when both CAA and CERAD are considered. The participant with no NPs (participant A) had a low DVR. Three participants with moderate NPs had a DVR greater than 1.2 in at least 1 CERAD region. In the middle frontal gyrus, 2 participants with moderate NPs had a DVR greater than 1.2. For the inferior parietal lobule and the SMTG, only 1 participant with moderate plaques had a DVR greater than 1.2. Discordance between CERAD and regional DVR remained apparent in 2 individuals. In participant E, who had predominantly diffuse plaques on pathologic evaluation, a high DVR was again observed in the setting of sparse NPs. The regional DVR remained less than 1.2 in participant B, despite moderate NPs in all 3 CERAD regions.

[^{11}C]PiB Retention in Relation to Quantitative Aβ Load—Detectable Aβ using immunohistochemical analysis was found at a DVR greater than 1.2 in the precuneus, with increasing DVRs as Aβ levels increased (Figure 6).

COMMENT

We examined the relation between in vivo Aβ load assessed by means of [^{11}C]PiB and postmortem neuropathologic evaluation of NPs according to CERAD criteria.[6] In individuals with either minimal or globally elevated in vivo Aβ load, amyloid imaging was in agreement with postmortem assessment. In individuals with either intermediate or localized elevation of Aβ levels in vivo, variable agreement with diagnostic neuropathologic assessment was observed, even after applying several thresholds for PiB+ and accounting for CAA.

The observation of agreement between imaging and CERAD plaque rating in an individual with globally elevated [^{11}C]PiB retention before and after dementia diagnosis is consistent with case reports of demented patients who underwent imaging using [^{11}C]PiB and autopsy.[2,5] This finding suggests that agreement between imaging and postmortem assessment of NPs demonstrated with silver stains is likely in the presence of a greatly elevated Aβ load.

We also observed agreement between imaging and pathologic findings in an older adult who had undetectable Aβ on in vivo imaging and no evidence of NPs or CAA on diagnostic neuropathologic evaluation. This individual may best represent situations in which “negative PiB” studies may be useful for the exclusion of elevated Aβ load. In the present series, however, there were also older adults with minimally elevated or localized Aβ loads on in vivo imaging who had moderate numbers of NPs (ie, CERAD B). Furthermore, we observed increased [^{11}C]PiB retention in a CAA-positive participant with low NP burden but extensive Aβ detectable by means of immunohistochemical analysis.

In this group of 6 individuals with in vivo imaging and postmortem evaluation, in vivo amyloid imaging showed limited overall agreement with CERAD NP ratings. Agreement was maximized in 5 of 6 participants using a DVR threshold of 1.2 and considering NPs and CAA. This corresponds with the level of PiB detectability of Aβ in the precuneus, one of the earliest regions of increased [^{11}C]PiB retention.[21] In addition, good agreement between in vivo imaging and pathologic findings is seen when only CAA is considered, consistent with reports of [^{11}C]PiB as a CAA tracer.[1,3]

Potential factors that may affect the relation between in vivo imaging and CERAD-based assessment of NPs fall into 3 broad categories: (1) those related to CERAD's semi-quantitative assessment of Aβ, (2) those related to different forms of Aβ, and (3) other factors, such as the imaging–pathologic assessment interval. The CERAD rating is based on a small volume of tissue and it is determined by the highest number of NPs in a single high-power field in any 1 of 3 cortical regions examined. In contrast, in vivo amyloid imaging quantifies Aβ in the entire brain on a continuous scale, with the mean DVR across 8 cortical regions used for evaluation. These differences are especially important in the evaluation of nondemented older adults in whom accumulation of Aβ is initially observed in regions such as the precuneus and the anterior cingulate,[21] regions that are not included in the CERAD assessment. Best illustrated by participant E in this series, in vivo imaging studies of the entire brain can inform more regionally targeted neuropathologic investigations.

Differences in the type of Aβ may also contribute to the limited agreement between in vivo amyloid imaging and diagnostic neuropathologic assessment.[4,7] Carbon 11–labeled PiB binds to fibrillar Aβ deposits not only in NPs but also in diffuse (albeit with lower affinity)[2,7] and cored[2] plaques and vascular amyloid,[1,3] which, unlike NPs, are not included in the CERAD neuropathologic diagnostic evaluation. Furthermore, although immunostaining with anti-Aβ antibodies can be used for quantitative assessment of plaques and CAA, such immunostains, are not used in the CERAD-based neuropathologic assessment. A polymorphic form of Aβ, to which [^{11}C]PiB does not bind,[22] may potentially account for some cases in which moderate NPs are observed using neuropathologic assessment despite low cortical [^{11}C]PiB retention. It is possible that these "PiB-refractory" forms of Aβ are more common early in the course of Aβ deposition, such as that seen in cognitively healthy individuals.

Other factors, such as the interval between in vivo imaging and neuropathologic evaluation, may also potentially affect the agreement between in vivo imaging and CERAD assessment, especially in those with an Aβ load near the PiB+ threshold. Tritiated PiB or 6-CN-PiB stain[2] may provide an alternative way to compare PiB and plaque burden at autopsy.[2]

This study has several limitations. Larger samples of older adults with both [^{11}C]PiB imaging and postmortem assessment would improve our understanding of the relation between imaging and pathologic findings, especially in subgroups such as those with asymptomatic AD (individuals with AD pathology but no clinical impairment).[11] In addition, the interval between [^{11}C]PiB imaging and autopsy is variable. However, this study represents the largest series of older adults to date with both in vivo imaging and neuropathologic assessment,[2,5,7] and it is the only series that includes nondemented older adults. In addition, a decade of prospective neuropsychological follow-up and consensus diagnosis, especially in the participant with 3 in vivo [^{11}C]PiB studies who progressed to dementia, provides a unique opportunity to better understand how cognitive changes relate to Aβ load in vivo. Such prospective studies will be critical in guiding the timing of preventive therapies. More detailed investigations of [^{11}C]PiB retention in relation to immunohistochemical quantification of regional Aβ load in more brain areas and continued

longitudinal imaging studies are ongoing and will provide important information on the extent to which amyloid imaging detects abnormality early in the disease process.

Acknowledgments

Funding/Support: This research was supported in part by the Intramural Research Program of the National Institute on Aging, National Institutes of Health, and N01-AG-3-2124 and extramural grants K24 DA00412 (Dr Wong), P50 AG005133, R37 AG025516 (Dr Klunk), and P01 AG025204 (Dr Klunk) and by grant P50 AG05146 from The Johns Hopkins University Alzheimer's Disease Research Center.

References

1. Lockhart A, Lamb JR, Osredkar T, et al. PIB is a non-specific imaging marker of amyloid-beta (Aβ) peptide-related cerebral amyloidosis. Brain. 2007; 130(pt 10):2607–2615. [PubMed: 17698496]
2. Ikonomovic MD, Klunk WE, Abrahamson EE, et al. Post-mortem correlates of *in vivo* PiB-PET amyloid imaging in a typical case of Alzheimer's disease. Brain. 2008; 131(pt 6):1630–1645. [PubMed: 18339640]
3. Johnson KA, Gregas M, Becker JA, et al. Imaging of amyloid burden and distribution in cerebral amyloid angiopathy. Ann Neurol. 2007; 62(3):229–234. [PubMed: 17683091]
4. Leinonen V, Alafuzoff I, Aalto S, et al. Assessment of β-amyloid in a frontal cortical brain biopsy specimen and by positron emission tomography with carbon 11–labeled Pittsburgh Compound B. Arch Neurol. 2008; 65(10):1304–1309. [PubMed: 18695050]
5. Bacskai BJ, Frosch MP, Freeman SH, et al. Molecular imaging with Pittsburgh Compound B confirmed at autopsy: a case report. Arch Neurol. 2007; 64(3):431–434. [PubMed: 17353389]
6. Mirra SS, Hart MN, Terry RD. Making the diagnosis of Alzheimer's disease: a primer for practicing pathologists. Arch Pathol Lab Med. 1993; 117(2):132–144. [PubMed: 8427562]
7. Cairns NJ, Ikonomovic MD, Benzinger T, et al. Absence of Pittsburgh compound B detection of cerebral amyloid β in a patient with clinical, cognitive, and cerebrospinal fluid markers of Alzheimer disease: a case report. Arch Neurol. 2009; 66(12):1557–1562. [PubMed: 20008664]
8. Aizenstein HJ, Nebes RD, Saxton JA, et al. Frequent amyloid deposition without significant cognitive impairment among the elderly. Arch Neurol. 2008; 65(11):1509–1517. [PubMed: 19001171]
9. Resnick SM, Goldszal AF, Davatzikos C, et al. One-year age changes in MRI brain volumes in older adults. Cereb Cortex. 2000; 10(5):464–472. [PubMed: 10847596]
10. Kawas C, Gray S, Brookmeyer R, Fozard J, Zonderman A. Age-specific incidence rates of Alzheimer's disease: the Baltimore Longitudinal Study of Aging. Neurology. 2000; 54(11):2072–2077. [PubMed: 10851365]
11. Driscoll I, Resnick SM, Troncoso JC, An Y, O'Brien R, Zonderman AB. Impact of Alzheimer's pathology on cognitive trajectories in nondemented elderly. Ann Neurol. 2006; 60(6):688–695. [PubMed: 17192929]
12. Petersen RC. Mild cognitive impairment: current research and clinical implications. Semin Neurol. 2007; 27(1):22–31. [PubMed: 17226738]
13. Price JC, Klunk WE, Lopresti BJ, et al. Kinetic modeling of amyloid binding in humans using PET imaging and Pittsburgh Compound–B. J Cereb Blood Flow Metab. 2005; 25(11):1528–1547. [PubMed: 15944649]
14. Zhou Y, Resnick SM, Ye W, et al. Using a reference tissue model with spatial constraint to quantify [^{11}C]Pittsburgh compound B PET for early diagnosis of Alzheimer's disease. Neuroimage. 2007; 36(2):298–312. [PubMed: 17449282]
15. Zhou Y, Endres CJ, Brasić JR, Huang S-C, Wong DF. Linear regression with spatial constraint to generate parametric images of ligand-receptor dynamic PET studies with a simplified reference tissue model. Neuroimage. 2003; 18(4):975–989. [PubMed: 12725772]
16. Rorden C, Brett M. Stereotaxic display of brain lesions. Behav Neurol. 2000; 12(4):191–200. [PubMed: 11568431]

17. Yamamoto T, Hirano A. A comparative study of modified Bielschowsky, Bodian and thioflavin S stains on Alzheimer's neurofibrillary tangles. Neuropathol Appl Neurobiol. 1986; 12(1):3–9. [PubMed: 2422580]

18. Braak H, Braak E. Neuropathological stageing of Alzheimer-related changes. Acta Neuropathol. 1991; 82(4):239–259. [PubMed: 1759558]

19. McKeith IG, Galasko D, Kosaka K, et al. Consensus guidelines for the clinical and pathologic diagnosis of dementia with Lewy bodies (DLB): report of the consortium on DLB international workshop. Neurology. 1996; 47(5):1113–1124. [PubMed: 8909416]

20. Roe CM, Mintun MA, D'Angelo G, Xiong C, Grant EA, Morris JC. Alzheimer disease and cognitive reserve: variation of education effect with carbon 11–labeled Pittsburgh Compound B uptake. Arch Neurol. 2008; 65(11):1467–1471. [PubMed: 19001165]

21. Mintun MA, Larossa GN, Sheline YI, et al. [^{11}C]PIB in a nondemented population: potential antecedent marker of Alzheimer disease. Neurology. 2006; 67 (3):446–452. [PubMed: 16894106]

22. Rosen RF, Ciliax BJ, Wingo TS, et al. Deficient high-affinity binding of Pittsburgh compound B in a case of Alzheimer's disease. Acta Neuropathol. 2010; 119(2):221–233. [PubMed: 19690877]

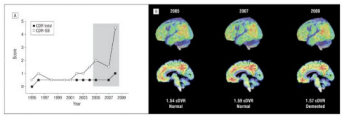

Figure 1.
Longitudinal in vivo carbon 11–labeled Pittsburgh Compound B ([^{11}C]PiB) imaging in an older adult with cognitive decline. A, Informant Clinical Dementia Rating (CDR) scores before and during in vivo β-amyloid imaging. The shaded area shows CDR data at the time of the [^{11}C]PiB studies shown in part B. B, Surface projections and parasagittal [^{11}C]PiB images during the participant's cognitive decline. Consensus diagnoses and mean cortical distribution volume ratios (cDVRs) are noted below the images. Neuropathologic findings for this individual are shown in Figure 4F. CDR-SB indicates CDR Sum of Boxes.

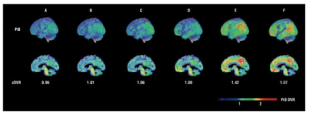

Figure 2.
In vivo β-amyloid load in older adults. Voxelwise in vivo carbon 11–labeled Pittsburgh Compound B (PiB) distribution volume ratios (DVR) overlaid on cortical surface and parasagittal sections allowing comparison with neuropathologic Consortium to Establish a Registry for AD assessment. Participants are marked A to F to correspond to the data in the tables, text, and other figures.

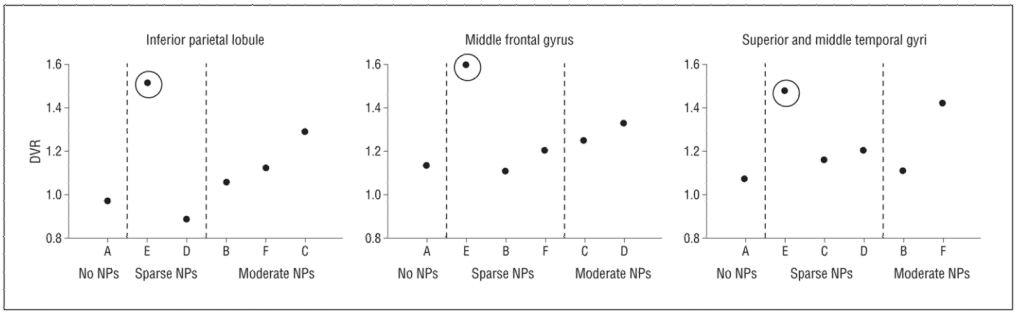

Figure 3.

In vivo carbon 11–labeled Pittsburgh Compound B imaging and Consortium to Establish a Registry for AD (CERAD) assessment of neuritic plaques (NPs). Participant E, with fibrillar β-amyloid (Aβ) primarily in diffuse plaques, is identified by circles. Participant A has a low distribution volume ratio (DVR) and no NPs. Three participants with moderate NPs have a DVR greater than 1.2 in at least 1 of the CERAD regions. Participants are marked A to F to correspond to the data in the tables, text, and other figures.

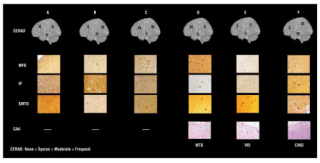

Figure 4.
Consortium to Establish a Registry for AD (CERAD) assessment of neuritic plaques (NPs) in older adults with antemortem in vivo carbon 11–labeled Pittsburgh Compound B imaging. The CERAD plaque rating (N indicates no NPs; S, sparse NPs; and M, moderate NPs) in the middle frontal gyrus (MFG), inferior parietal lobule (IP), and superior and middle temporal gyri (SMTG) of Hirano-stained tissue sections is noted on cortical surface projection (original magnification ×100). The presence or absence of cerebral amyloid angiopathy (CAA) is noted (original magnification ×200). In participant F, CAA is also found in the visual cortex (VIS). Participants are marked A to F to correspond to the data in the tables, text, and other figures. CING indicates cingulate gyrus; MTG, middle temporal gyrus.

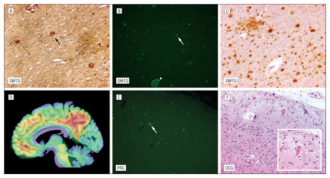

Figure 5.
Potential factors limiting agreement between in vivo β-amyloid imaging and diagnostic neuropathologic assessment, illustrated for participant E. A, β-Amyloid (Aβ) load in the neuritic plaque (black arrow) in the superior and middle temporal gyri (SMTG) (Hirano, original magnification ×100). B, Fibrillar Aβ in diffuse plaques (white arrow) and blood vessel wall (arrowhead) in the SMTG (thioflavin S, original magnification ×100). C, The Aβ load by immunohistochemical analysis in the SMTG (6E10 antibody, original magnification ×100). D, Sagittal parametric carbon 11–labeled Pittsburgh Compound B image overlaid on a magnetic resonance image shows a high Aβ load in the precuneus. E, Fibrillar Aβ load in diffuse plaques (white arrow) in the precuneus (PRC) not routinely evaluated by Consortium to Establish a Registry for AD assessment (thioflavin S, original magnification ×100). F, Cerebral amyloid angiopathy in the occipital gyrus (OCG) (hematoxylineosin, original magnification ×100) (inset: original magnification ×200).

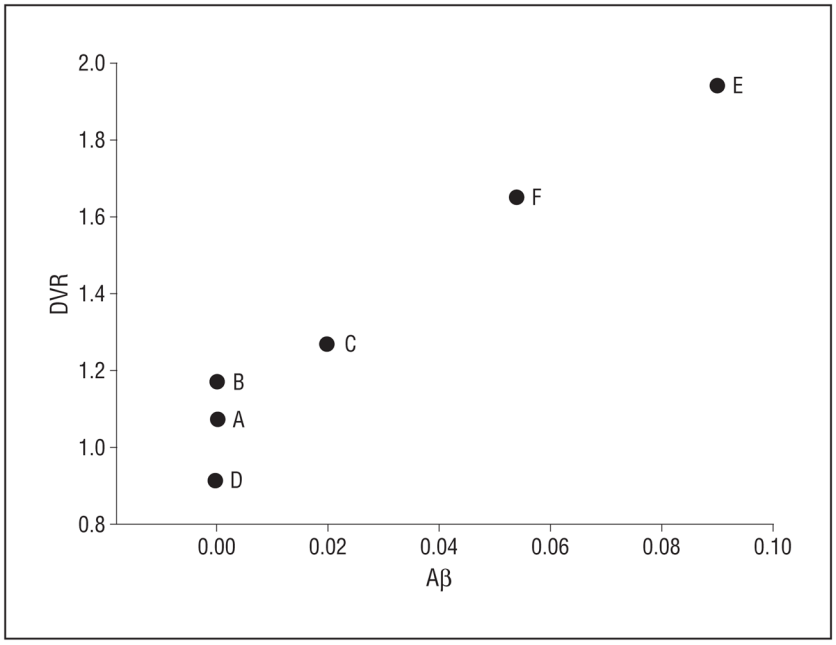

Figure 6.
In vivo carbon 11–labeled Pittsburgh Compound B and β-amyloid (Aβ) levels by immunohistochemical analysis in the precuneus. Aβ reflects percentage area in which Aβ is detected by 6E10 antibody. A detectable level of Aβ is observed at a distribution volume ratio (DVR) greater than 1.2. Participants are marked A to F to correspond to the data in the tables, text, and other figures.

Table 1

Demographic, Genetic, and Cognitive Data

	Participants							
Variable	**A**	**B**	**C**	**D**	**E**	**F1**	**F2**	**F3**
Demographics								
Age at [^{11}C]PiB PET, y	80	78	79	87	85	80	82	84
Sex	M	F	M	M	M		M	
Education, y	19	18	15	18	16	20	20	20
Genetics								
Family history of dementia	−	−	+	−	−		+	
Apolipoprotein E genotype, alleles	33	34	23	33	33		34	
Cognitive status at imaging								
CDR	0	0	0	0.5	0	0.5	0.5	1.0
CDR-SB	0	0	0	0.5	0	2.0	1.5	4.5
Neuropsychological testing								
MMSE score	30	30	29	25	30	30	30	30
Memory								
CVLT immediate recall (maximum=80)	79	75	34	16[a]	56	60	NA	NV
CVLT delayed recall (maximum=16)	16	16	9	0[a]	14	10	NA	NV
BVRT errors	2	9	11	1[a]	5	8	7	10
Cued selective reminding immediate (maximum=48)	37	39	23	29	37	31	21	25
Cued selective reminding delayed (maximum=16)	15	14	14	11	9	ND	10	6
Slope CVLT immediate recall[b]	0.75	0.04	−0.28[c]	−1.54[c]	0.25		−0.32[c]	
Executive function								
Trails A, s (No. of errors)	19 (0)	34 (0)	55 (0)	50 (0)	27 (0)	43 (0)	59 (0)	44 (0)
Trails B, s (No. of errors)	53 (0)	59 (0)	116 (0)	78 (0)	92 (3)	140 (0)	147 (1)	144 (1)
Language, No. of words recalled								
Category fluency	45	53	36	24	41	54	35	30
Letter fluency	39	59	20	41	58	49	58	24
Boston Naming Test (No. of correct spontaneous responses, maximum=60)	59	59	57	55	56	57	56	46

Abbreviations: BVRT, Benton Visual Retention Test; [^{11}C]PiB, carbon 11–labeled Pittsburgh Compound B; CDR, Clinical Dementia Rating Scale; CDR-SB, CDR Sum of Boxes; CVLT, California Verbal Learning Test; MMSE, Mini-Mental State Examination; NA, not available; NV, not valid; PET, positron emission tomography; −, not present; +, present.

[a] Last data available 1.5 years before imaging.

[b] Slope CVLT immediate recall is the rate of change across time.

[c] Indicates a significant decline across time.

Table 2

In Vivo β-Amyloid Load and Diagnostic Neuropathologic Assessment

	Participants							
Variable	**A**	**B**	**C**	**D**	**E**	**F1**	**F2**	**F3**
Amyloid load: overall								
Imaging								
Mean cDVR	0.96	1.01	1.06	1.09	1.42	1.54	1.59	1.57
Highest regional DVR	1.03	1.16	1.24	1.21	2.07	1.93	2.00	1.90
Pathologic assessment								
CERAD NP rating	None	Moderate	Moderate	Moderate	Sparse	Moderate	Moderate	Moderate
Amyloid angiopathy	No	No	No	Yes	Yes	Yes	Yes	Yes
Amyloid load: regional								
Imaging (DVR)								
Orbitofrontal	0.93	0.96	0.92	1.12	1.27	1.49	1.54	1.58
Prefrontal	0.86	0.93	0.93	1.21	1.26	1.52	1.60	1.63
Superior frontal	0.95	0.99	1.06	1.22[a]	1.39	1.67	1.69	1.67
Parietal	0.94	0.96	1.07	0.94	1.42	1.40	1.44	1.42
Lateral temporal	0.94	0.98	1.01	1.11	1.28	1.39	1.42	1.43
Medial temporal	1.00	1.04	1.02	0.95	1.13	0.94	0.90	0.90
Occipital	1.01	1.08	1.02	1.03	1.18	1.09	1.11	1.14
Anterior cingulate	1.00	1.03	1.22	1.21	1.48	1.84	1.88	1.78
Posterior cingulate	1.03[a]	1.16[a]	1.24[a]	0.91	2.07[a]	1.93[a]	2.00[a]	1.90[a]
Pathologic findings								
Middle frontal gyrus	None	Sparse	Moderate	Moderate	Sparse		Sparse	
Inferior parietal gyrus	None	Moderate	Moderate	Sparse	Sparse		Moderate	
Superior and middle temporal gyri	None	Moderate	Sparse	Sparse	Sparse		Moderate	
Neuropathologic assessment								
CERAD rating (overall)	0	B	B	B	A		B	
Braak (Stage)	4	3	4	3	4		3	
NIA-Reagan criteria for likelihood of dementia	Not met	Not met	Not met	Intermediate	Not met		Intermediate	
Neuropathologic diagnosis of AD (CERAD)	Normal	Possible AD	Possible AD	Possible AD	Normal		Probable AD	

	Participants							
Variable	**A**	**B**	**C**	**D**	**E**	**F1**	**F2**	**F3**
Imaging–pathologic assessment interval, y	1.7	2.4	2.4	1.1	1.4	3.1	1.8	0.2
Postmortem delay, h	36	13	15	7.5	>48		22	
Other pathologic findings								
Lewy bodies	None	None	None	None	Yes		None	
Infarcts	None	No	Yes	None	None		None	
Microinfarcts	Cerebellar cortex	No	No	None	Caudate		None	
Atherosclerosis	Yes	Yes	Yes	Yes	Yes		Yes	

Abbreviations: AD, Alzheimer disease; cDVR, cortical distribution volume ratio; CERAD, Consortium to Establish a Registry for AD; DVR, distribution volume ratio; NIA, National Institute on Aging; NP, neuritic plaque.

[a] Indicates the highest regional DVR.

Table 3

Agreement of Fibrillar β-Amyloid Detected by [^{11}C]PiB Imaging and Diagnostic Neuropathologic Assessment

	CERAD ≥ Moderate			CAA+			CERAD ≥ Moderate or CAA+		
[^{11}C]PiB+ Cutoff Point	**CP**	**CN**	**Overall Agreement**	**CP**	**CN**	**Overall Agreement**	**CP**	**CN**	**Overall Agreement**
Mean cDVR: 1.4	1/4	1/2	2/6	2/3	3/3	5/6	2/5	1/1	3/6
Highest regional DVR: 1.4	1/4	1/2	2/6	2/3	3/3	5/6	2/5	1/1	3/6
DVR in the highest CERAD region: 1.4	1/4	1/2	2/6	2/3	3/3	5/6	2/5	1/1	3/6
Mean cDVR: 1.3	1/4	1/2	2/6	2/3	3/3	5/6	2/5	1/1	3/6
Highest regional DVR: 1.3	1/4	1/2	2/6	2/3	3/3	5/6	2/5	1/1	3/6
DVR in the highest CERAD region: 1.3	2/4	1/2	3/6	3/3	3/3	6/6	3/5	1/1	4/6
Mean cDVR: 1.2	1/4	1/2	2/6	2/3	3/3	5/6	2/5	1/1	3/6
Highest regional DVR: 1.2	3/4	1/2	4/6	3/3	2/3	5/6	4/5	1/1	5/6
DVR in the highest CERAD region: 1.2	3/4	1/2	4/6	3/3	2/3	5/6	4/5	1/1	5/6

Abbreviations: [^{11}C]PiB, carbon 11–labeled Pittsburgh Compound B; cDVR, cortical [^{11}C]PiB distribution volume ratio; CAA, cerebral amyloid angiopathy; CERAD, Consortium to Establish a Registry for Alzheimer Disease (a semiquantitative neuropathologic scale used for the assessment of neuritic plaque load); CN, CERAD negative; CP, CERAD positive; DVR, distribution volume ratio.